

Radial orthogonality and Lebesgue constants on the disk

Annie Cuyt · Irem Yaman ·
Bayram Ali Ibrahimoglu · Brahim Benouahmane

Received: 20 December 2011 / Accepted: 20 June 2012 /
Published online: 4 July 2012
© Springer Science+Business Media, LLC 2012

Abstract In polynomial interpolation, the choice of the polynomial basis and the location of the interpolation points play an important role numerically, even more so in the multivariate case. We explore the concept of spherical orthogonality for multivariate polynomials in more detail on the disk. We focus on two items: on the one hand the construction of a fully orthogonal cartesian basis for the space of multivariate polynomials starting from this sequence of spherical orthogonal polynomials, and on the other hand the connection between these orthogonal polynomials and the Lebesgue constant in multivariate polynomial interpolation on the disk. We point out the many links of the two topics under discussion with the existing literature. The new results are illustrated with an example of polynomial interpolation and approximation on the unit disk. The numerical example is also compared with the popular radial basis function interpolation.

A. Cuyt · B. A. Ibrahimoglu
Department of Mathematics and Computer Science, Universiteit Antwerpen (CMI),
Middelheimlaan 1, 2020 Antwerpen, Belgium

A. Cuyt
e-mail: annie.cuyt@ua.ac.be

I. Yaman (✉)
Department of Mathematics, Faculty of Science, Gebze Institute of Technology,
Çayirova Campus, 41400 Gebze Kocaeli, Turkey
e-mail: i.yaman@gyte.edu.tr

B. A. Ibrahimoglu
Department of Mathematical Engineering, Yıldız Technical University,
Davutpasa Campus, 34210 Istanbul, Turkey

B. Benouahmane
Département de Mathématiques, Faculté des Sciences et Techniques,
Université Hassan II, BP 146 Yasmina, 20650 Mohammadia, Morocco

Keywords Polynomial interpolation · Lebesgue constant · Orthogonal polynomials · Unit disk · Several variables

1 Introduction

The choice of a polynomial basis and the location of the interpolation points greatly influence the numerical conditioning of polynomial interpolation, and hence the quality of the computed interpolant. Moreover, some sets of interpolation points deliver near-best polynomial approximants, while others lead to divergence of the interpolation scheme. Fortunately, a univariate polynomial basis is always a Chebyshev system, thereby guaranteeing the existence and unicity of the polynomial interpolant for a set of distinct interpolation points.

In the multivariate case, the situation is much more difficult. The location of the interpolation points also needs to be such that it guarantees unisolvence of the interpolation problem because no polynomial basis is a Chebyshev system. And because of the curse of dimensionality faced in polynomial interpolation, alternative techniques like radial basis interpolation have become very popular. But then the latter are prone to ill-conditioning. Here we propose an extremely well-conditioned alternative to radial basis interpolation on the disk (see Sections 3 and 4). At the same time we identify sets of interpolation points that guarantee a very small Lebesgue constant and consequently interpolants that are near-best polynomial approximants (see Sections 5 and 6).

Both results follow from a detailed study of radial or spherical orthogonality on the disk.

2 The Lebesgue constant

Let the function f belong to $C([-1, 1])$. When approximating f by an element from a finite-dimensional $C_n = \text{span}\{\phi_0, \dots, \phi_n\}$ with $\phi_i \in C([-1, 1])$ for $0 \leq i \leq n$, we know that there exists at least one element p_n^* in C_n that is closest to f . This element is the unique closest one if the ϕ_0, \dots, ϕ_n are a Chebyshev system. Since the computation of this element is more complicated than that of the interpolant

$$\sum_{i=0}^n a_i \phi_i(x_j) = f(x_j), \quad j = 0, \dots, n, \quad -1 \leq x_j \leq 1,$$

scientists have looked for interpolation points x_j that make the infinity or Chebyshev norm

$$\left\| f(x) - \sum_{i=0}^n a_i \phi_i(x) \right\|_{\infty}$$

of the interpolation error as small as possible on the unit interval $[-1, 1]$.

When $\phi_i(x) = x^i$ (or another polynomial basis) then for the interpolant

$$p_n(x) = \sum_{i=0}^n a_i x^i,$$

satisfying $p_n(x_j) = f(x_j), 0 \leq j \leq n$, with the x_j distinct, the error $\|f - p_n\|_\infty$ is bounded by

$$\|f - p_n\|_\infty \leq \max_{x \in [-1, 1]} \left(\frac{|f^{(n+1)}(x)|}{(n+1)!} \right) \max_{x \in [-1, 1]} \prod_{j=0}^n |x - x_j|.$$

Interpolation in distinct points is sufficient to guarantee the existence and uniqueness of the polynomial interpolant. In addition, it is well-known that the monic $(x - x_0) \cdots (x - x_n)$ is minimal if the x_j are the zeroes of the $(n + 1)$ -th degree Chebyshev polynomial of the first kind $T_{n+1}(x) = \cos((n + 1) \arccos x)$, satisfying the orthogonality

$$\int_{-1}^1 T_i(x) T_{n+1}(x) \frac{1}{\sqrt{1-x^2}} dx = 0, \quad i = 0, \dots, n.$$

In later sections we also encounter the Chebyshev polynomials of the second kind $U_{n+1}(x)$ which satisfy the orthogonality

$$\int_{-1}^1 U_i(x) U_{n+1}(x) \sqrt{1-x^2} dx = 0, \quad i = 0, \dots, n.$$

The procedure that associates with f its interpolant p_n is linear and given by

$$P_n : C([-1, 1]) \rightarrow C_n : f(x) \rightarrow p_n(x) = \sum_{i=0}^n f(x_i) \ell_i(x)$$

where the basic Lagrange polynomials $\ell_i(x)$,

$$\ell_i(x) = \prod_{j=0, j \neq i}^n \frac{x - x_j}{x_i - x_j},$$

satisfy $\ell_i(x_j) = \delta_{ij}$. Hence another bound for the interpolation error is given by

$$\|f - p_n\|_\infty \leq (1 + \|P_n\|) \|f - p_n^*\|_\infty, \quad \|P_n\| = \max_{x \in [-1, 1]} \sum_{i=0}^n |\ell_i(x)|.$$

Here $\Lambda_n := \Lambda_n(x_0, \dots, x_n) = \|P_n\|$ is called the Lebesgue constant and it depends on the location of the interpolation points x_j . So it is clear that we prefer interpolation points x_0, \dots, x_n that guarantee us a small Lebesgue constant.

The Lebesgue constant also expresses the conditioning of the polynomial interpolation problem in the Lagrange basis. Let $\tilde{p}_n(x)$ denote the polynomial interpolant of degree n for the perturbed function \tilde{f} in the same interpolation points:

$$\tilde{p}_n(x) = \sum_{i=0}^n \tilde{f}(x_i) \ell_i(x).$$

Since $\|p_n\|_\infty \geq \max_{i=0,\dots,n} |f(x_i)|$ we have

$$\begin{aligned} \frac{\|p_n - \tilde{p}_n\|_\infty}{\|p_n\|_\infty} &\leq \frac{\max_{x \in [-1,1]} \sum_{i=0}^n |f(x_i) - \tilde{f}(x_i)| |\ell_i(x)|}{\max_{i=0,\dots,n} |f(x_i)|} \\ &\leq \Lambda_n(x_0, \dots, x_n) \frac{\max_{i=0,\dots,n} |f(x_i) - \tilde{f}(x_i)|}{\max_{i=0,\dots,n} |f(x_i)|}. \end{aligned} \tag{1}$$

Other useful bases to formulate the polynomial interpolation problem in, are the orthogonal polynomial bases, among which the already mentioned Chebyshev polynomials. It is well-known that in the monomial basis the condition number can grow exponentially fast [9]. Let $V_n(x_0, \dots, x_n)$ denote the Vandermonde matrix of size $n + 1$ constructed with the points x_0, \dots, x_n . Then for $x_j \in [-1, 1]$,

$$\|V_n(x_0, \dots, x_n)\|_\infty \|V_n^{-1}(x_0, \dots, x_n)\|_\infty \leq (n + 1) \max_{0 \leq i \leq n} \left(\prod_{j=0, j \neq i}^n \frac{1 + |x_j|}{|x_j - x_i|} \right)$$

with equality if the x_j all lie in $[0, 1]$ or $[-1, 0]$.

An explicit formula for the x_j that minimize the Lebesgue constant is not known, and if no further constraints are imposed on the interpolation points then the solution is not even unique. But it is proved in [15] that the minimal growth of the Lebesgue constant in terms of the degree n is given by $(2/\pi) \log(n + 1) + (2/\pi) (\gamma + \log(4/\pi)) \approx (2/\pi) \log(n + 1) + 0.52125 \dots$ with γ the Euler constant.

Several node sets x_0, \dots, x_n come close to realizing this minimal growth, among which the already mentioned Chebyshev zeroes of $T_{n+1}(x)$,

$$\Lambda_n(x_0, \dots, x_n) < \frac{2}{\pi} \log(n + 1) + 0.97343 \dots, \quad n \geq 1.$$

The node set known in closed form that approximates the optimal node set best is probably the so-called extended Chebyshev node set given by

$$x_j = -\frac{\cos\left(\frac{(2j+1)\pi}{2(n+1)}\right)}{\cos\left(\frac{\pi}{2(n+1)}\right)}, \quad j = 0, \dots, n. \tag{2}$$

The division by $\cos(\pi/(2n + 2))$ guarantees that $x_0 = -1$ and $x_n = 1$, an idea that plays a role in Section 5 too. The growth of the Lebesgue constant for the extended Chebyshev nodes is bounded by [11]

$$\Lambda_n(x_0, \dots, x_n) < \frac{2}{\pi} \log(n + 1) + 0.5829 \dots, \quad n \geq 4.$$

In our search for interpolation node sets in closed form that give small bivariate Lebesgue constants on the disk, we depart from the close connection between orthogonal polynomials and Lebesgue constants. To this end we need the so-called radial or spherical orthogonality for multivariate polynomials. In Section 3 this concept is introduced in the d -variate space \mathbb{R}^d . In the Sections 4 and 5 we further explore the bivariate case $d = 2$. The spherically orthogonal polynomials also give rise to an optimally conditioned basis for numerical work on the disk. This result is established in Section 4 and illustrated in Section 7.

3 Radial orthogonality

Let $\overline{B}_{d,p}(0; 1)$ denote the closed unit ball centered at the origin in \mathbb{R}^d equipped with the ℓ_p -norm. For each ℓ_p -norm this ball is a d -variate analogue of the closed interval $[-1, 1]$. For $p = \infty$ and $d = 2$ it is the unit square $[-1, 1] \times [-1, 1]$, for $p = 2$ and $d = 2$ the unit disk $\{(x, y); 0 \leq x^2 + y^2 \leq 1\}$ and for $p = 1$ and $d = 2$ it is the simplex $\{(x, y); 0 \leq |x| + |y| \leq 1\}$.

For the definition of our multivariate orthogonal polynomials we replace the cartesian coordinates $X = (x_1, \dots, x_d) \in \mathbb{R}^d$ by the new spherical coordinates $X = (x_1, \dots, x_d) = (\lambda_1 z, \dots, \lambda_d z)$ with $\lambda = (\lambda_1, \dots, \lambda_d)$ belonging to the ℓ_p unit sphere $S_{d,p}(0; 1) \subset \mathbb{R}^d$ and $z \in \mathbb{R}$. While λ contains the directional information of X , the radial variable z contains the signed distance information. A signed distance function is defined by

$$\text{sd}(X) = \text{sgn}(x_k) \|X\|_p, \quad k = \min\{j : x_j \neq 0\}. \tag{3}$$

Since λ is not unique for a given X , we choose it such that for given X we have $z = \text{sd}(X)$. We denote by $\mathbb{R}[\lambda] = \mathbb{R}[\lambda_1, \dots, \lambda_d]$ the linear space of d -variate polynomials in the λ_k with real coefficients, by $\mathbb{R}(\lambda) = \mathbb{R}(\lambda_1, \dots, \lambda_d)$ the commutative field of rational functions in the λ_k with real coefficients, by $\mathbb{R}[\lambda][z]$ the linear space of polynomials in the variable z with coefficients from $\mathbb{R}[\lambda]$ and by $\mathbb{R}(\lambda)[z]$ the linear space of polynomials in the variable z with coefficients from $\mathbb{R}(\lambda)$.

In the bivariate case we mostly use the notation $X = (x, y)$ instead of $X = (x_1, x_2)$ and $\lambda = (\alpha, \beta)$ instead of $\lambda = (\lambda_1, \lambda_2)$.

We introduce d -variate functions $V_m(X)$ that are polynomials in z with coefficients from $\mathbb{R}[\lambda]$:

$$V_m(X) = \mathcal{V}_m(\lambda; z) = \sum_{i=0}^m b_{m^2-i}(\lambda) z^i.$$

The $b_{m^2-i}(\lambda)$ are homogeneous polynomials in the λ_k of degree $m^2 - i$. Note that the functions $V_m(X)$ do not belong to $\mathbb{R}[X]$ but they belong to $\mathbb{R}[\lambda][z]$. Therefore the $V_m(X)$ can be viewed as spherical polynomials: for every $\lambda \in S_{d,p}(0; 1)$ the function $V_m(X) = \mathcal{V}_m(\lambda; z)$ is a polynomial of degree m in the spherical variable $z = \text{sd}(X)$. In addition, the functions

$$\mathcal{V}_m(\lambda; \lambda_1 x_1 + \dots + \lambda_d x_d), \quad \lambda \in S_{d,p}(0; 1), \quad X \in \mathbb{R}^d$$

are polynomial in the x_k , they belong to $\mathbb{R}[\lambda][X]$ and play a crucial role in the sequel. Here the vectors λ and X are symbolic and can vary independently of each other: X need not belong to $\text{span}\{\lambda\}$.

On the $\mathcal{V}_m(\lambda; \lambda_1 x_1 + \dots + \lambda_d x_d)$ we impose the orthogonality conditions

$$\int \dots \int_{\|X\|_p \leq 1} \left(\sum_{k=1}^d x_k \lambda_k \right)^i \mathcal{V}_m \left(\lambda; \sum_{k=1}^d x_k \lambda_k \right) w(z) dX = 0, \quad i = 0, \dots, m - 1 \tag{4}$$

where $w(z)$ is a non-negative weight function with

$$\int \dots \int_{\|X\|_p \leq 1} w(z) dX < \infty, \quad z = \text{sd}(X).$$

The coefficients $b_{m^2-i}(\lambda)$ are obtained from the (symbolic/parameterized) linear system

$$\sum_{j=0}^m c_{i+j}(\lambda) b_{m^2-j}(\lambda) = 0, \quad i = 0, \dots, m - 1 \tag{5}$$

where $c_i(\lambda)$ are the moments given by

$$c_i(\lambda) = \int \dots \int_{\|X\|_p \leq 1} \left(\sum_{k=1}^d x_k \lambda_k \right)^i w(z) dX, \quad i = 0, \dots, 2m - 1. \tag{6}$$

The $c_i(\lambda)$ are homogeneous polynomials in the λ_k of degree i . This radial or spherical orthogonality was already introduced in [1] and [2] although it was not yet termed like that in the early references. An explanation why $b_{m^2-i}(\lambda)$ needs to be of degree $m^2 - i$ is also given there.

For a fixed directional vector $\lambda = \lambda^*$, the projected spherical polynomials $\mathcal{V}_m(\lambda^*; \lambda_1^* x_1 + \dots + \lambda_d^* x_d)$ are univariate polynomials in the variable $z = \lambda_1^* x_1 + \dots + \lambda_d^* x_d$, orthogonal on the interval $[A, B] \subset \text{span}\{\lambda^*\}$ with

$$A = \min_{(x_1, \dots, x_d) \in \overline{B}_{d,p}(0; 1)} (\lambda_1^* x_1 + \dots + \lambda_d^* x_d), \quad B = \max_{(x_1, \dots, x_d) \in \overline{B}_{d,p}(0; 1)} (\lambda_1^* x_1 + \dots + \lambda_d^* x_d) \tag{7}$$

and $\lambda^* \in S_{d,p}(0; 1)$. Note that the weight function is multivariate instead of univariate. In addition, the weight at $X = (x_1, \dots, x_d) \in \overline{B}_{d,p}(0; 1)$ is $w(\text{sd}(X))$

with $z = \text{sd}(X)$ and $-1 \leq z \leq 1$ and not $w(\lambda_1^*x_1 + \dots + \lambda_d^*x_d)$ which has a different support.

We point out the similarity of the $\mathcal{V}_m(\lambda; \lambda_1x_1 + \dots + \lambda_dx_d)$ with radial basis functions. The variable of our multidimensional function is

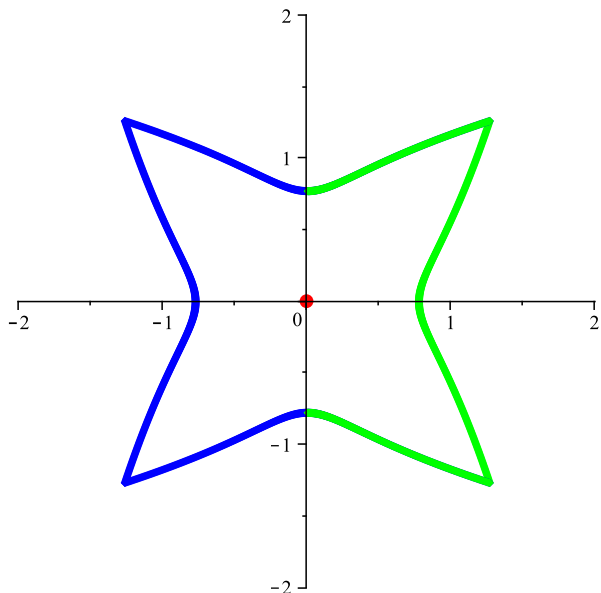
$$\langle X, \lambda \rangle = \lambda_1x_1 + \dots + \lambda_dx_d \tag{8}$$

which is the projection of X onto a directional unit vector $\lambda \in S_{d,p}(0; 1)$ and this for continuously varying λ . When $X \in \text{span}\{\lambda\}$, then $\langle X, \lambda \rangle = z\|\lambda\|_2^2$. In the case of radial basis functions the variable is a weighted $\|X - C\|_p$ for a set of distinct vectors C . So for the user the choice is between spherical orthogonality or radial functions forming a Chebyshev set. More on the comparison with radial basis functions is to be found in Section 7.

For symmetric weight functions $w(z)$, the zeroes $\zeta_{i,m}(\lambda), i = 1, \dots, m$ of the spherical orthogonal polynomials $\mathcal{V}_m(\lambda; z)$ appear in symmetric pairs, with one zero describing a curve in the right halfplane because of (3) and the other zero tracking the same curve in the left halfplane but mirrored with respect to the origin. In Fig. 1 we show the zeroes for the case $d = 2, p = \infty, m = 3$ and $w(z) = 1$: $\zeta_{1,3}(\lambda)$ lies in the left half plane, $\zeta_{2,3}(\lambda)$ equals zero, $\zeta_{3,3}(\lambda)$ lies in the right half plane. For $\lambda^* = (1, 1)$ for instance, the zeroes $\zeta_{1,3}(\lambda^*), \zeta_{2,3}(\lambda^*), \zeta_{3,3}(\lambda^*)$ lie in the interval $[-2, 2]$ which is the support of orthogonality in $\text{span}\{(1, 1)\}$.

In the case of Theorem 2 below, each curve $\zeta_{i,m}(\lambda)$ is a half circle, unlike in Fig. 1. So a symmetric pair of zeroes describes a full circle. We then simply say that the radius of the circle equals the zero of the spherical orthogonal

Fig. 1 Zero curves of $\mathcal{V}_3(\lambda; z)$ orthogonal on $\overline{B}_{2,\infty}(0; 1)$ for $w(z) = 1$



polynomial, and this is to be understood as a positive and a negative zero each describing half a circle. A use of this can be found in Section 5.

Note that for the moment the functions $V_m(X) = \mathcal{V}_m(\lambda; z)$ are unnormalized. We usually normalize them by requiring that $\gcd(b_{m^2-m}(\lambda), \dots, b_{m^2}(\lambda)) = 1$, thus decreasing the degree of the $b_{m^2-i}(\lambda)$ with the same amount for each i . When the $b_{m^2-i}(\lambda)$ reduce to a constant, then the $V_m(X) = \mathcal{V}_m(\lambda; z)$ can be made monic. Examples of $V_m(X) = \mathcal{V}_m(\lambda; z)$ for different weight functions are given in [8].

4 Bivariate orthogonal cartesian basis

Now assume that $d=2$, in other words we are considering the ℓ_p -ball $\overline{B}_{2,p}(0; 1)$, and denote $\lambda_1 = \alpha$ and $\lambda_2 = \beta$. When substituting actual values for the λ_k then the function $\mathcal{V}_m(\lambda; \lambda_1 x_1 + \dots + \lambda_d x_d)$ becomes a polynomial function in the x_k . The question that arises is whether these radially orthogonal functions can be used to construct a cartesian orthogonal basis for the linear space $\mathbb{R}[X]$. The answer is affirmative and the proof goes in three steps. Theorem 1 applies to general weight functions $w(z)$ and all ℓ_p -norms. Theorem 2 holds for specific weight functions and the closed Euclidean d -ball $\overline{B}_{d,2}(0; 1)$. Theorem 3 is only valid for the specific weight function $w(z) = 1$ on the Euclidean disk $\overline{B}_{2,2}(0; 1)$.

Theorem 1 *The set $\{\mathcal{V}_m(\alpha_{m,k}, \beta_{m,k}; \alpha_{m,k}x + \beta_{m,k}y), 0 \leq k \leq m, m \in \mathbb{N}\}$ is a basis for $\mathbb{R}[x, y]$ if*

$$\begin{vmatrix} \alpha_{m,0}^m & \alpha_{m,0}^{m-1} \beta_{m,0} & \cdots & \alpha_{m,0} \beta_{m,0}^{m-1} & \beta_{m,0}^m \\ \alpha_{m,1}^m & \alpha_{m,1}^{m-1} \beta_{m,1} & \cdots & \alpha_{m,1} \beta_{m,1}^{m-1} & \beta_{m,1}^m \\ \vdots & \vdots & & \vdots & \vdots \\ \alpha_{m,m}^m & \alpha_{m,m}^{m-1} \beta_{m,m} & \cdots & \alpha_{m,m} \beta_{m,m}^{m-1} & \beta_{m,m}^m \end{vmatrix} \neq 0, \quad m \in \mathbb{N}.$$

Proof It suffices to prove that for each m the $(\alpha_{m,k}x + \beta_{m,k}y)^m$ with $k = 0, \dots, m$ are a basis for the homogeneous polynomials of degree m in x and y . So let us assume that a nontrivial vector $(\gamma_0, \dots, \gamma_m)$ exists such that

$$\sum_{k=0}^m \gamma_k (\alpha_{m,k}x + \beta_{m,k}y)^m = 0.$$

Then

$$\sum_{i=0}^m \binom{m}{i} x^{m-i} y^i \left(\sum_{k=0}^m \gamma_k \alpha_{m,k}^{m-i} \beta_{m,k}^i \right) = 0$$

and hence

$$\sum_{k=0}^m \gamma_k \alpha_{m,k}^{m-i} \beta_{m,k}^i = 0, \quad i = 0, \dots, m.$$

But the latter is impossible because of the regularity of the coefficient matrix

$$A = (a_{i+1,k+1})_{0 \leq i,k \leq m} = (\alpha_{m,k}^{m-i} \beta_{m,k}^i)_{0 \leq i,k \leq m}.$$

□

An appropriate selection for the values $\alpha_{m,k}$ and $\beta_{m,k}$ is for instance

$$\alpha_{m,k} = \frac{k}{\|(k, m - k)\|_p}, \quad \beta_{m,k} = \frac{m - k}{\|(k, m - k)\|_p}.$$

So with $\mathcal{V}_m(\lambda; z)$ computed for a general weight function $w(z)$, the functions

$$\begin{aligned} &1 \\ &\mathcal{V}_1((1, 0); x) \\ &\mathcal{V}_1((0, 1); y) \\ &\mathcal{V}_2((2, 0)/\|(2, 0)\|_p; x) \\ &\mathcal{V}_2((1, 1)/\|(1, 1)\|_p; (x + y)/\|(1, 1)\|_p) \\ &\mathcal{V}_2((0, 2)/\|(0, 2)\|_p; y) \\ &\vdots \end{aligned} \tag{9}$$

provide a basis for the bivariate polynomials, but not yet an orthogonal basis. We now indicate how this can be achieved. In the sequel we focus on the Euclidean norm ($p = 2$) and we consider weight functions of the form

$$w(z) = (1 - z^2)^{v-1/2}, \quad v > -1/2, \tag{10}$$

because this class is large enough for our purpose. The following result holds in d dimensions.

Theorem 2 *For $w(z)$ given by (10) the radial polynomials $\mathcal{V}_m(\lambda; z)$ are independent of λ and we have the additional orthogonality*

$$\begin{aligned} &\int \dots \int_{\|X\|_2 \leq 1} \mathcal{V}_i\left(\cdot; \sum_{k=1}^d x_k \mu_k\right) \mathcal{V}_m\left(\cdot; \sum_{k=1}^d x_k \lambda_k\right) w(z) dX \\ &= \begin{cases} 0, & i = 0, \dots, m - 1, \\ \frac{\pi^{d/2}(2v + d - 1)\Gamma(v + 1/2)}{(2v + 2m + d - 1)\Gamma(v + (d + 1)/2)} \mathcal{V}_m\left(\cdot; \sum_{k=1}^d \lambda_k \mu_k\right), & i = m. \end{cases} \end{aligned}$$

Proof For the polynomials $\mathcal{V}_m(\lambda; \lambda_1 x_1 + \dots + \lambda_d x_d)$ satisfying the orthogonality conditions (4) with $w(z)$ given by (10) and a continuous function f defined on $[-1, 1]$ the Funk–Hecke formula in [16] gives

$$\begin{aligned} & \int \dots \int_{\|X\|_2 \leq 1} f(\mu_1 x_1 + \dots + \mu_d x_d) \mathcal{V}_m(\lambda; \lambda_1 x_1 + \dots + \lambda_d x_d) (1 - z^2)^{\nu-1/2} dX \\ &= \frac{\pi^{(d-1)/2} \Gamma(\nu + 1/2)}{C_m^{\nu+(d-1)/2}(1) \Gamma(\nu + d/2)} \mathcal{V}_m(\lambda; \lambda_1 \mu_1 + \dots + \lambda_d \mu_d) \\ & \times \int_{-1}^1 f(t) C_m^{\nu+(d-1)/2}(t) (1 - t^2)^{\nu-1+d/2} dt \end{aligned}$$

where $C_m^{(\nu)}(z)$ are the univariate Gegenbauer polynomials orthogonal with respect to the weight $(1 - z^2)^{\nu-1/2}$ on $[-1, 1]$. For the moments $c_i(\lambda)$ defined by (6) we thus obtain with $f(t) = t^i$, $\mu = \lambda$ and $m = 0$ that

$$\begin{aligned} c_i(\lambda) &= \int \dots \int_{\|X\|_2 \leq 1} (\lambda_1 x_1 + \dots + \lambda_d x_d)^i (1 - z^2)^{\nu-1/2} dX \\ &= \frac{\pi^{(d-1)/2} \Gamma(\nu + 1/2)}{\Gamma(\nu + d/2)} \int_{-1}^1 t^i (1 - t^2)^{\nu-1+d/2} dt. \end{aligned}$$

Since these $c_i(\lambda)$ do not depend on λ , the coefficients solved from (5) do not either and so we can write

$$\mathcal{V}_m(\lambda; z) = \mathcal{V}_m(\cdot; z).$$

At the same time we see that the moments $c_0(\cdot), c_1(\cdot), c_2(\cdot), \dots$ equal up to the factor

$$\frac{\Gamma(\nu + 1/2) \pi^{(d-1)/2}}{\Gamma(\nu + d/2)}$$

the moments of the univariate Gegenbauer polynomials $C_m^{\nu+(d-1)/2}(z)$. Hence we can also write

$$\mathcal{V}_m(\cdot; z) = \left(\frac{\Gamma(\nu + 1/2) \pi^{(d-1)/2}}{\Gamma(\nu + d/2)} \right)^m C_m^{\nu+(d-1)/2}(z).$$

The expressions for the integral in the proposition follow from the Funk–Hecke formula in a similar way, now with

$$f(t) = C_i^{\nu+(d-1)/2}(t).$$

□

The above theorem guarantees the orthogonality of polynomials of different degree irrespective of the choice of λ , which may indeed be different when the degrees differ as in (9). In other words, with the $\mathcal{V}_m(\lambda; z)$ orthogonal with

respect to the weight function $w(z) = (1 - z^2)^{\nu-1/2}$ on the Euclidean disk, each of the $m + 1$ functions $\mathcal{V}_m(\cdot; \alpha_{m,k}x + \beta_{m,k}y)$ of degree m is orthogonal to each of the $i + 1$ functions $\mathcal{V}_i(\cdot; \alpha_{i,k}x + \beta_{i,k}y)$ of degree i . So the functions $\mathcal{V}_1(\cdot; x)$ and $\mathcal{V}_1(\cdot; y)$ are orthogonal to the functions $\mathcal{V}_2(\cdot; x)$, $\mathcal{V}_2(\cdot; (x + y)/\sqrt{2})$, $\mathcal{V}_2(\cdot; y)$. Let us now deal with the remaining problem, being that of the mutual orthogonality of the $m + 1$ polynomials of degree m on each other.

Theorem 3 *The set $\{\mathcal{V}_m(\alpha_{m,k}, \beta_{m,k}; \alpha_{m,k}x + \beta_{m,k}y), 0 \leq k \leq m, m \in \mathbb{N}\}$ with $\alpha_{m,k} = \cos(k\pi/(m + 1))$ and $\beta_{m,k} = \sin(k\pi/(m + 1))$ is an orthogonal basis for $\mathbb{R}[x, y]$ with respect to the weight function $w(z) = 1$.*

Proof The proclaimed result can be obtained from [16]. But a separate proof is immediate now and goes as follows. From Theorem 2 we know that functions of different degree are orthogonal because the weight function has the form (10) with $\nu = 1/2$. We also know that different functions of equal degree are only orthogonal if

$$\mathcal{V}_m\left(\cdot; \sum_{k=1}^d \lambda_k \mu_k\right) = 0.$$

Since for $w(z) = 1$ the $\mathcal{V}_m(\cdot; z)$ coincide up to a factor with the Gegenbauer polynomials $C_m^{(1)}(z)$ we need to have

$$\lambda_1 \mu_1 + \lambda_2 \mu_2 = \alpha_{m,k} \alpha_{m,\ell} + \beta_{m,k} \beta_{m,\ell} = \cos(i\pi/(m + 1))$$

for some $i = 1, \dots, m$ and whatever $0 \leq k, \ell \leq m, k \neq \ell$ which is satisfied for the above $\alpha_{k,m}$ and $\beta_{k,m}$. □

So with $\mathcal{V}_m(\cdot; z)$ orthogonal with respect to the weight function $w(z) = 1$ on the Euclidean disk, the polynomials

$$\begin{aligned} &1 \\ &\mathcal{V}_1(\cdot; x) \\ &\mathcal{V}_1(\cdot; y) \\ &\mathcal{V}_2(\cdot; x) \\ &\mathcal{V}_2(\cdot; x \cos \pi/3 + y \sin \pi/3) \\ &\mathcal{V}_2(\cdot; x \cos 2\pi/3 + y \sin 2\pi/3) \\ &\vdots \end{aligned} \tag{11}$$

are a fully orthogonal basis on $\overline{B}_{2,2}(0; 1)$ for $\mathbb{R}[x, y]$. In Section 7 we give an illustration of the use of this basis in least squares approximation.

5 Small Lebesgue constants on the disk

When moving to more than one variable, we face some immediate problems since

$$\text{span} \{1, x, y, x^2, xy, y^2, \dots\}$$

is not a Chebyshev system anymore. So an additional concern in polynomial interpolation is the unsolvence of the interpolation problem. Unless otherwise indicated, we consider polynomials of full homogeneous degree. In two variables this means that a polynomial of degree n has the form

$$p_n(x, y) = \sum_{i+j=0}^n a_{ij}x^i y^j$$

with $N + 1 = (n + 1)(n + 2)/2$ coefficients. We consider the interpolation problem

$$p_n(x_k, y_k) = f(x_k, y_k), \quad k = 0, \dots, N, \quad (x_k, y_k) \in \overline{B}_{2,p}(0; 1).$$

Let $\{\phi_0, \dots, \phi_N\} = \{x^i y^j; 0 \leq i + j \leq n\}$ and let $\{(x_k, y_k); 0 \leq k \leq N\}$ be such that the matrix

$$V_N = (\Phi_{\ell+1,k+1})_{(N+1) \times (N+1)}, \quad \Phi_{\ell+1,k+1} = \phi_k(x_\ell, y_\ell), \quad 0 \leq \ell, k \leq N$$

is regular. The node sets that we consider in the sequel always guarantee this. Then the polynomial interpolant can be written as

$$p_n(x, y) = \sum_{i=0}^N f(x_i, y_i) \ell_i(x, y)$$

with

$$\ell_i(x, y) = \frac{\det V_{N,i}}{\det V_N},$$

where the matrix $V_{N,i}$ equals the matrix V_N except that the i -th row is replaced by $(\phi_0(x, y), \dots, \phi_N(x, y))$. With the functions $\ell_i(x, y)$ we define the Lebesgue constant

$$\Lambda_n^{(2)} := \Lambda_n((x_0, y_0), \dots, (x_N, y_N)) = \max_{(x,y) \in \overline{B}_{2,p}(0;1)} \sum_{i=0}^N |\ell_i(x, y)|.$$

The minimal growth of $\Lambda_n^{(2)}$ is different for different ℓ_p -balls. For instance, on the square the minimal order of growth is $O(\ln^2(n + 1))$ and this order is achieved for the configurations of interpolation points given in [5] and [6].

On the disk the minimal order of growth is quite different, namely $O(\sqrt{n + 1})$, as proved in [14]. No configurations of interpolation points obeying this order of growth are known. We analyze the Lebesgue constant on the disk for different unisolvent configurations and present the best that can be obtained so far.

On the simplex the minimal order of growth is not even known. Instead, in [10] some (non closed form) configurations of interpolation points are obtained from the solution of a minimization problem. There is clearly a lot of interest in the problem.

Several configurations of interpolation points on concentric circles guarantee unisolvence on the disk. Among others we mention [4, 13, 17]. We tried all configurations but report here only on the closed form set that gives the smaller Lebesgue constant $\Lambda_n^{(2)}$ on the disk. As can be expected, it is a configuration that increases the number of interpolation points towards the boundary.

Let us divide a total of $\lfloor n/2 \rfloor + 1$ concentric circles with center at the origin into k groups,

$$v_1 + \dots + v_k = \left\lfloor \frac{n}{2} \right\rfloor + 1, \quad v_i \in \mathbb{N}, \quad i = 1, \dots, k,$$

with the j -th group containing v_j circles with respective radii $r_1^{(j)}, \dots, r_{v_j}^{(j)}$. On each circle in the j -th group we take the same number of $2n_j + 1$ equidistant interpolation points where

$$\begin{aligned} n_1 &= n - v_1 + 1, \\ n_2 &= n - 2v_1 - v_2 + 1, \\ &\vdots \\ n_k &= n - 2v_1 - \dots - 2v_{k-1} - v_k + 1. \end{aligned}$$

Then it is easy to see that

$$v_1(2n_1 + 1) + \dots + v_k(2n_k + 1) = N + 1$$

and that the Lebesgue constant $\Lambda_n^{(2)}$ decreases if k increases, for the simple reason that the points become more uniformly distributed over the circles as k approaches $\lfloor n/2 \rfloor + 1$ with $v_j = 1$ for $j = 1, \dots, \lfloor n/2 \rfloor + 1$. In [4] it is proved that this configuration of points is unisolvent on the disk. For which of the larger k exactly the minimal value of $\Lambda_n^{(2)}$ is attained, depends on the interplay between the radii of the concentric circles and the distribution of the interpolation points over the disk. Smaller Lebesgue constants can be expected if the Dubiner distance between the interpolation points varies less [7]. We return to this issue in Section 6.

Remains the problem of how to choose the radii. In the Figs. 2, 3, 4 and 5 we have taken the radii equal to the extended zeroes of the spherical Legendre polynomials, where this has to be interpreted as explained at the end of

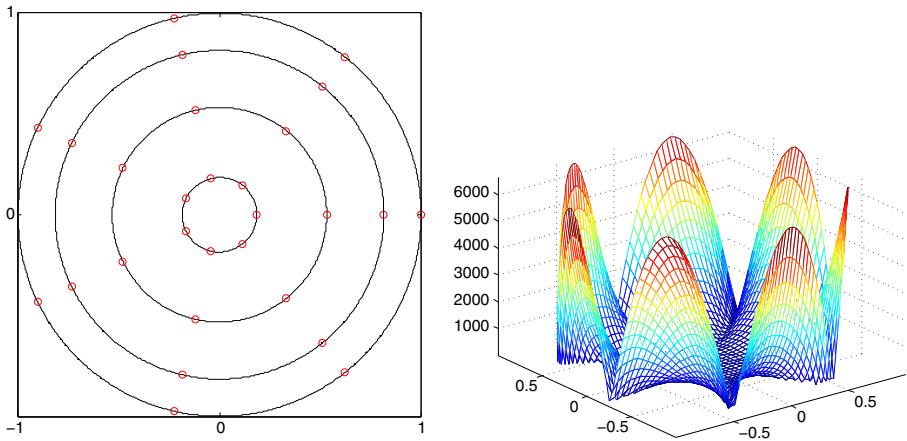


Fig. 2 Case $k = 1$

Section 3. We illustrate this for $n = 6$ and $N + 1 = 28$. We point out that additional rotations with respect to each other of the concentric circles containing the interpolation points, have an effect on the Lebesgue constant under study, but never to the point that its order of magnitude for a certain configuration (meaning a certain value for k) is altered. A decrease of the Lebesgue constant due to such rotations is only marginal.

In Fig. 2 one finds the case $k = 1$, so $v_1 = 4$ with $n_1 = 3$, where the 28 interpolation points are distributed over 4 concentric circles each containing 7 equidistant points. The Lebesgue constant in this case is a whopping 6648. In Fig. 3 the number k is increased to 2 and we take $v_1 = 2$, $v_2 = 2$, so 11 points on each of the 2 outer circles and 3 points on each of the 2 inner circles.

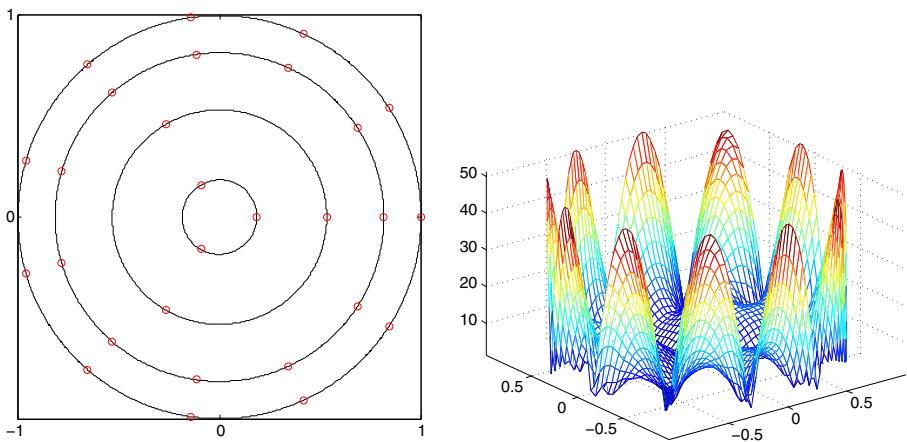


Fig. 3 Case $k = 2$

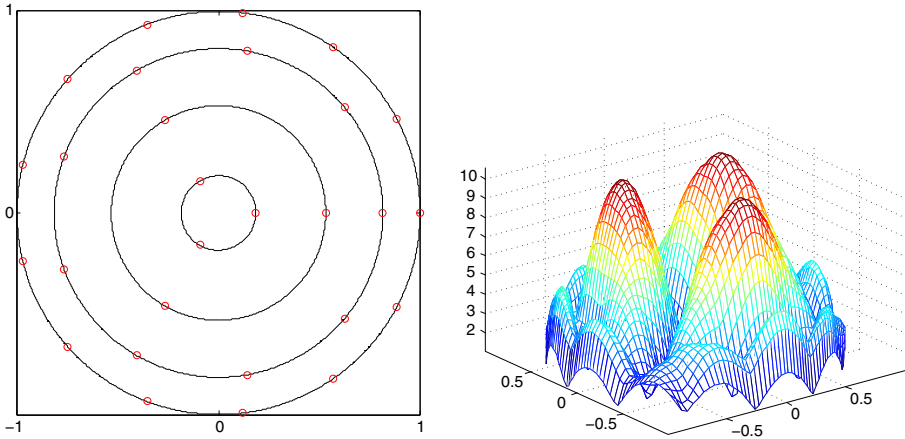


Fig. 4 Case $k = 3$

This clearly improves the Lebesgue constant to about 51.17. In Fig. 4 we take $k = 3$ with $\nu_1 = 1, \nu_2 = 1, \nu_3 = 2$, so 13 interpolation points on the outer circle, another circle with 7 points and 3 interpolation points on each of the 2 inner circles. The Lebesgue constant is further going down to approximately 10.58. Finally with $k = 4$ and all $\nu_j = 1$ for $j = 1, \dots, 4$ the Lebesgue constant is smallest, namely 4.68. We have respectively 13, 9 and 5 interpolation points on 3 concentric circles and the last point at the origin. We repeat that the radii in the Figs. 2–5 are taken as the extended zeroes of the spherical Legendre polynomials of respective degrees 8, 8, 8 and 7.

In Fig. 6 we illustrate that the growth rate of the Lebesgue constant $\Lambda_n^{(2)}$ is slowest for this choice: we compare the Lebesgue constants for the radii

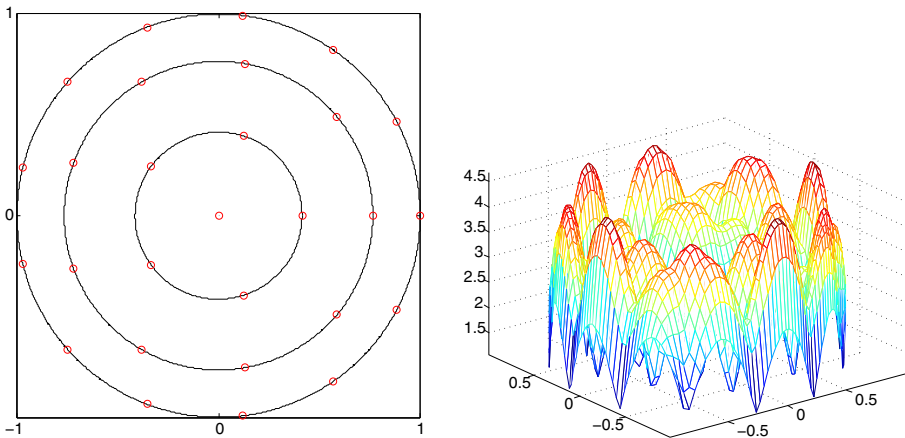
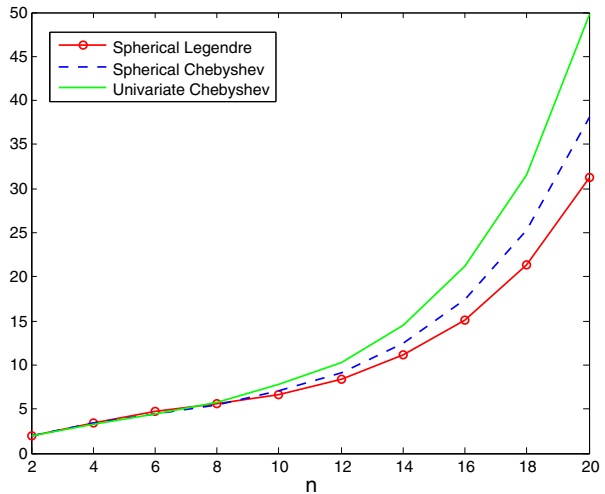


Fig. 5 Case $k = 4$

Fig. 6 Growth of $\Lambda_n^{(2)}$ for $k = \lfloor n/2 \rfloor + 1$



being the extended zeroes of the spherical Legendre, the extended zeroes of the spherical Chebyshev and the extended zeroes of the univariate Chebyshev polynomials, the latter being given by (2). Unless otherwise mentioned, Chebyshev polynomials are of the first kind, in other words orthogonal with respect to the weight function $w(z) = 1/\sqrt{1 - z^2}$. For each degree n we have immediately taken k to be the maximal value $\lfloor n/2 \rfloor + 1$.

6 Exploring other configurations on the disk

The configurations leading to Lebesgue constants with minimal growth on the square $\overline{B}_{2,\infty}(0; 1)$ (see [5] and [6]) are slightly different from the above. We now analyze whether similar configurations to the ones on the square can be considered on the disk and whether they are any good. Our point of departure are the so-called Padua points [7].

A first observation is that the $N + 1$ Padua interpolation points are distributed over the unit square on n concentric squares with increasing radius and with (from the center to the boundary) i points on the i -th square for $i = 1, \dots, n - 1$ and $2n + 1$ points on the n -th square, being the boundary of $\overline{B}_{2,\infty}(0; 1)$. Also, we show that the radii of the inner $n - 1$ concentric squares are the zeroes of the univariate Chebyshev polynomials of the second kind $U_n(z)$ and $U_{n-1}(z)$, excluding zero, where the symmetric zeroes are interpreted as in the Sections 2 and 4. To see this we organize the Padua interpolation points for degree n , explicated in [5] as

$$\left(x^{(j,k)} = (-1)^{j+k} \cos\left(\frac{j\pi}{n+1}\right), y^{(j,k)} = (-1)^{j+k} \cos\left(\frac{k\pi}{n}\right) \right), 0 \leq j + k \leq n,$$

in the following way. First we note that the points in

$$\begin{aligned}
 S_n = & \left\{ (-1)^{l+1} \left(\cos \left(\frac{l\pi}{n} \right), \cos \left(\frac{0\pi}{n+1} \right) \right) : l = 0, \dots, n \right\} \\
 \cup & \left\{ (-1)^{l+1} \left(\cos \left(\frac{0\pi}{n} \right), \cos \left(\frac{l\pi}{n+1} \right) \right) : l = 1, \dots, n \right\} \tag{12}
 \end{aligned}$$

lie on the boundary of the unit square. Then we take the collection of points consisting of

$$\begin{aligned}
 S_{n-i} = & \left\{ (-1)^{l+m+1} \left(\cos \left(\frac{l\pi}{n} \right), \cos \left(\frac{m\pi}{n+1} \right) \right) : m = \lceil i/2 \rceil, \right. \\
 & \left. l = m, \dots, n - m \right\}, \quad 1 \leq i \leq n - 1, i \text{ odd}
 \end{aligned}$$

$$\begin{aligned}
 S_{n-i} = & \left\{ (-1)^{l+m+1} \left(\cos \left(\frac{m\pi}{n} \right), \cos \left(\frac{l\pi}{n+1} \right) \right) : m = \lceil i/2 \rceil, \right. \\
 & \left. l = m + 1, \dots, n - m \right\}, \quad 1 \leq i \leq n - 1, i \text{ even}
 \end{aligned}$$

and lying on the same square of radius

$$\begin{aligned}
 \|(-1)^{l+m+1} (\cos(l\pi/n), \cos(m\pi/(n+1)))\|_\infty &= \cos(m\pi/(n+1)), & i \text{ odd,} \\
 \|(-1)^{l+m+1} (\cos(m\pi/n), \cos(l\pi/(n+1)))\|_\infty &= \cos(m\pi/n), & i \text{ even.}
 \end{aligned}$$

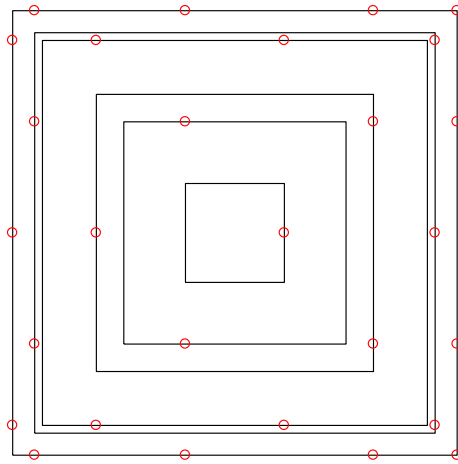
In Fig. 7 this is illustrated for $n = 6$. These ℓ_∞ radii are the zeroes of

$$\begin{aligned}
 U_n(z) &= \frac{\sin((n+1) \arccos(z))}{\sin(\arccos(z))}, \\
 U_{n-1}(z) &= \frac{\sin(n \arccos(z))}{\sin(\arccos(z))}.
 \end{aligned}$$

This explains why the radii are two by two rather similar, except for the innermost square that contains only one point.

When carrying this configuration to the disk, replacing concentric squares by concentric circles, copying the distribution of the points and the values of the radii, then what remains to specify is the distribution of the points on the i -th circle for $i = 1, \dots, n$. Here we can follow the simple rule that the points on the boundary of the unit disk are taken equidistantly and then (from the boundary to the center) the union of the points on each pair of concentric circles is also distributed equidistantly as if the points were lying on only one

Fig. 7 Padua points in $\overline{B}_{2,\infty}(0; 1)$ for $n = 6$



circle. Figure 8 for $n = 6$ illustrates this best. The accompanying Lebesgue constant $\Lambda_n^{(2)} = 7.76$. Another variation on this theme is to plainly take the set of the Padua points and map the square on the disk using

$$t(x, y) = \left(x \frac{\|(x, y)\|_\infty}{\|(x, y)\|_2}, y \frac{\|(x, y)\|_\infty}{\|(x, y)\|_2} \right), \quad (x, y) \in \overline{B}_{2,\infty}(0; 1).$$

For $n = 6$ this leads to the configuration in Fig. 9 with a matching Lebesgue constant of $\Lambda_6^{(2)} = 12.50$. Remember that smaller Lebesgue constants are to be expected from sets with a smaller variation in the Dubiner distance among the interpolation points [7]. The zeroes of the Chebyshev polynomials $T_{n+1}(x)$, for

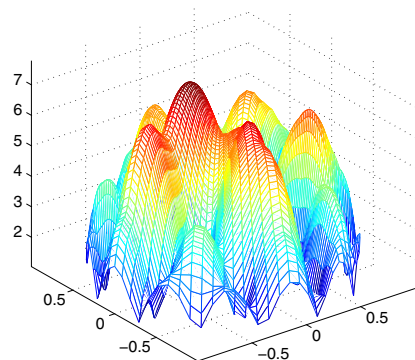
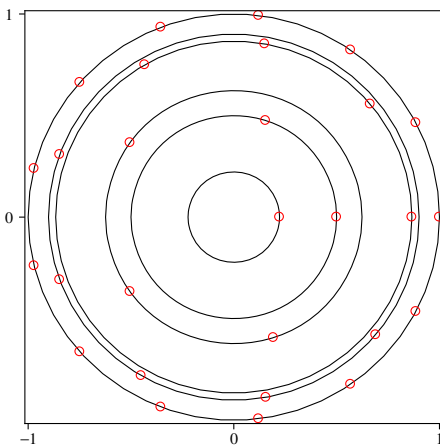


Fig. 8 Padua-like configuration on the disk for $n = 6$

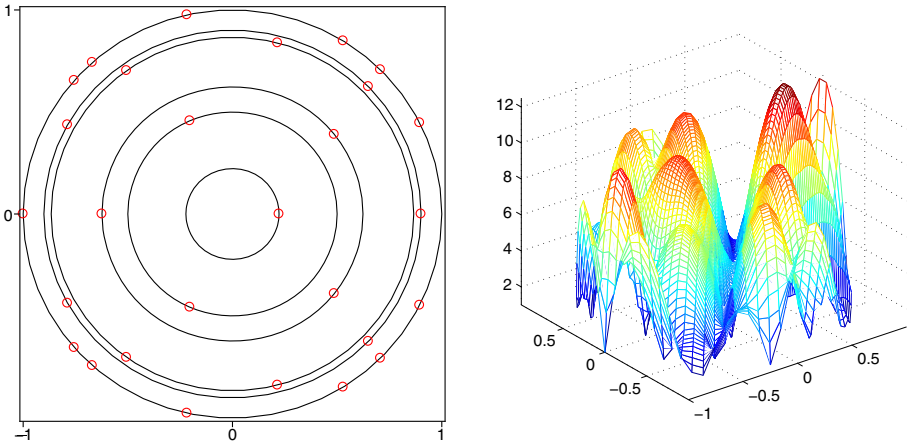


Fig. 9 Padua points for $n = 6$ mapped to the disk

instance, are equidistant with respect to the Dubiner distance. From this it is easy to conclude from Fig. 10 for $n = 33$, that the leftmost configuration which is the one described in Section 5, gives a smaller Lebesgue constant than the configuration in the middle, which is similar to that in Fig. 8, or the rightmost one, which is similar to that in Fig. 9. In the rightmost configuration there are clearly accumulations of interpolation points, while in the configuration in the middle the interpolation points are a bit too much pushed out of the center region.

Hence our conclusion that for small and moderate degrees ($n \leq 25$) the sets of interpolation points leading to the better Lebesgue constants on the disk are for the moment the ones given in Section 5. In parallel with our search, the authors of [3] were able to prove that unfortunately, even for a configuration of interpolation points laid out as in Fig. 5, the Lebesgue constant is doomed to blow up as n increases. But for practical interpolation purposes where the degree is reasonable, the configuration proposed here is the best known so far.

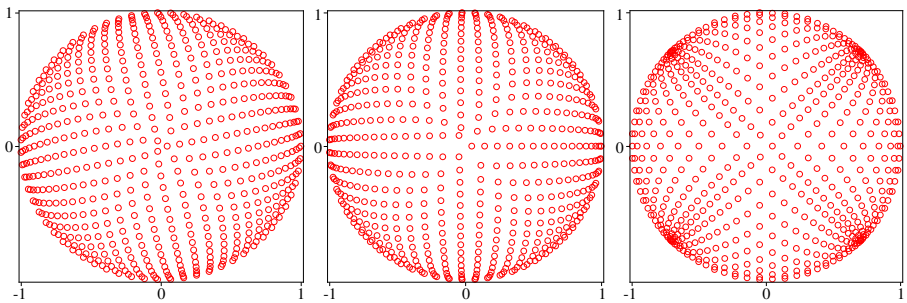


Fig. 10 Point configurations as in Figs. 5, 8 and 9 for $n = 33$

This is illustrated in Section 7 where the reader can compare, for various degrees n , the polynomial interpolant computed in the proposed set of interpolation points to the best polynomial approximant on the disk.

7 Illustration

Let $f(x, y)$ be the matlab peaks function (Fig. 11) on the Euclidean disk $\overline{B}_{2,2}(0; 1)$,

$$\begin{aligned}
 f(x, y) = & 3(1 - 3x)^2 \exp(-9x^2 - (3y + 1)^2) \\
 & - 10(3x/5 - 27x^3 - 243y^5) \exp(-9(x^2 + y^2)) \\
 & - (1/3) \exp(-(3x + 1)^2 - 9y^2), \quad (x, y) \in \overline{B}_{2,2}(0; 1).
 \end{aligned}$$

We illustrate the usefulness of the new orthogonal cartesian basis (11) derived in Section 4 and the configuration of interpolation points described in Section 5 with $k = \lfloor n/2 \rfloor + 1$, by computing on the one hand the least squares approximant to $f(x, y)$

$$\begin{aligned}
 q_n(x, y) &= \sum_{m=0}^n \sum_{k=0}^m v_{m,k} \mathcal{V}_m(\cdot; x \cos(k\pi/(m+1)) + y \sin(k\pi/(m+1))), \\
 v_{m,k} &= \frac{\int_{\overline{B}_{2,2}(0;1)} f(x, y) \mathcal{V}_m(\cdot; x \cos(k\pi/(m+1)) + y \sin(k\pi/(m+1))) dX}{\|\mathcal{V}_m(\cdot; x \cos(k\pi/(m+1)) + y \sin(k\pi/(m+1)))\|_2^2},
 \end{aligned}$$

Fig. 11 Graph of peaks function

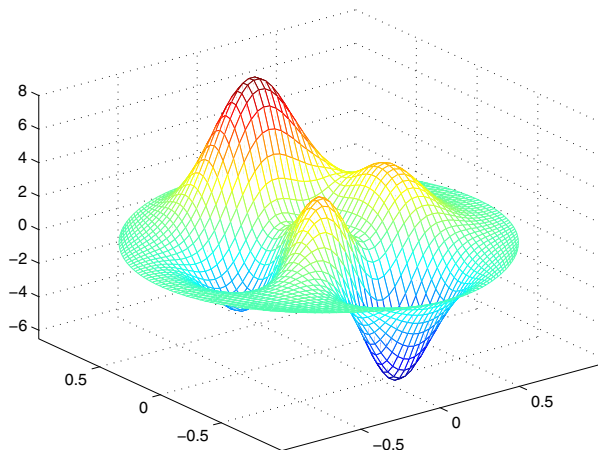


Table 1 ℓ_∞ errors of approximant $q_n(x, y)$, interpolant $p_n(x, y)$, and radial basis interpolants $r_n(x, y)$ and $s_n(x, y)$

n	$N + 1$	$\ f - q_n\ _\infty$	$\ f - p_n\ _\infty$	$\ f - r_n\ _\infty$	$\ f - s_n\ _\infty$
10	66	1.160	1.747	1.412	1.961
12	91	0.596	0.909	0.648	1.091
14	120	0.329	0.332	0.225	1.117
16	153	0.202	0.202	0.043	0.559
18	190	0.051	0.050	0.006	0.509
20	231	0.030	0.018	0.001	0.255

and on the other hand the polynomial interpolant of the same form with $v_{m,k}$ solved from the system of interpolation conditions

$$p_n(x_j, y_j) = f(x_j, y_j), \quad j = 0, \dots, N, \tag{13}$$

where the \mathcal{V}_m are the spherical Legendre polynomials on the Euclidean unit disk for $w(z) = 1$ and the interpolation points (x_j, y_j) are chosen similar to the configuration in Fig. 5. From Theorem 2 we easily find that

$$\begin{aligned} & \|\mathcal{V}_m(\cdot; x \cos(k\pi/(m + 1)) + y \sin(k\pi/(m + 1)))\|_2^2 \\ &= \int \int_{\overline{B}_{2,2}(0;1)} \mathcal{V}_m^2(\cdot; x \cos(k\pi/(m + 1)) + y \sin(k\pi/(m + 1))) \, dX = \pi. \end{aligned}$$

The polynomial $q_n(x, y)$ is the best ℓ_2 polynomial approximant for $f(x, y)$ on the disk $\overline{B}_{2,2}(0; 1)$. Due to the mutual orthogonality of all basis functions $\mathcal{V}_m(\cdot; x \cos(k\pi/(m + 1)) + y \sin(k\pi/(m + 1)))$ the coefficients $v_{m,k}$ do not have to be computed from a linear system. Instead, an explicit formula for the best polynomial approximant on the disk can now be written down.

Both p_n and q_n are also compared with the popular radial basis function interpolant [12]

$$r_n(x, y) = \sum_{k=0}^N \sigma_k \sqrt{1 + \|(x - x_k, y - y_k)\|_2^2}$$

Table 2 ℓ_2 errors of approximant $q_n(x, y)$ and interpolant $p_n(x, y)$

n	$N + 1$	$\ f - q_n\ _2$	$\ f - p_n\ _2$
10	66	0.494	0.717
12	91	0.251	0.377
14	120	0.134	0.182
16	153	0.058	0.081
18	190	0.014	0.025
20	231	0.007	0.009

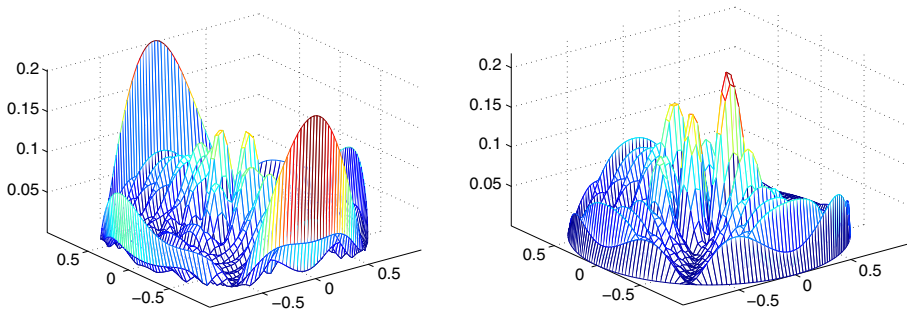


Fig. 12 Error plots of polynomial approximant $q_{16}(x, y)$ (left) and polynomial interpolant $p_{16}(x, y)$ (right)

and the (better conditioned but slower converging) constrained radial basis function interpolant [12]

$$s_n(x, y) = \sum_{k=0}^N \tau_k \|(x - x_k, y - y_k)\|_2^2 \ln(\|(x - x_k, y - y_k)\|_2)$$

where the constraint comes from adding a quadratic bivariate polynomial as described in [12]. In Table 1 we illustrate the errors $\|f - q_n\|_\infty, \|f - p_n\|_\infty, \|f - r_n\|_\infty$ and $\|f - s_n\|_\infty$ for different values of n . All errors were computed in higher precision (Maple) because of the ill-conditioning of the RBF interpolation problems. In Table 2 we give $\|f - q_n\|_2$ and $\|f - p_n\|_2$ and in Fig. 12 we show both the error curves $(q_{16} - f)(x, y)$ and $(p_{16} - f)(x, y)$. Note that the interpolant computed for the interpolation points constructed in Section 5 can indeed be called a near-best polynomial approximant, as one may expect from a set of good interpolation points.

In Table 3 one finds the condition numbers of the system of interpolation conditions (13) when written down using the new fully orthogonal basis compared to the use of:

- the classical tensor products $T_i(x)T_j(y)$ of Chebyshev polynomials,

Table 3 Condition number using mutually orthogonal basis versus tensor product basis and radial basis functions

n	$N + 1$	$\mathcal{V}_m(\cdot, \cdot)$	$T_i(x)T_j(y)$	$\sqrt{1 + (\cdot)^2}$	$(\cdot)^2 \ln(\cdot)$
10	66	$6.99e + 00$	$4.67e + 03$	$1.08e + 08$	$3.09e + 03$
12	91	$8.89e + 00$	$2.88e + 04$	$3.14e + 09$	$7.59e + 03$
14	120	$1.24e + 01$	$1.76e + 05$	$9.70e + 10$	$1.67e + 04$
16	153	$1.82e + 01$	$1.07e + 06$	$2.95e + 12$	$3.34e + 04$
18	190	$2.78e + 01$	$6.41e + 06$	$9.17e + 13$	$6.26e + 04$
20	231	$4.42e + 01$	$3.83e + 07$	$3.04e + 15$	$1.10e + 05$

- the radial basis functions $\sqrt{1 + \|(x - \cdot, y - \cdot)\|_2^2}$,
- the constrained radial basis functions $\|(x - \cdot, y - \cdot)\|_2^2 \ln(\|(x - \cdot, y - \cdot)\|_2)$,

where the constraints come from adding a quadratic bivariate polynomial. The results speak for themselves: the new basis gives extremely well-conditioned systems of interpolation conditions: on the disk the mutually orthogonal polynomials in (11) lead to far better conditioning than the orthogonal polynomials in (9) of which the conditioning is comparable to that of $T_i(x)T_j(y)$! And it is just a matter of choosing the directions λ in (8) wisely.

References

1. Benouahmane, B., Cuyt, A.: Multivariate orthogonal polynomials, homogeneous Padé approximants and Gaussian cubature. *Numer. Algorithms* **24**, 1–15 (2000). doi:[10.1023/A:1019128823463](https://doi.org/10.1023/A:1019128823463)
2. Benouahmane, B., Cuyt, A.: Properties of multivariate homogeneous orthogonal polynomials. *J. Approx. Theory* **113**(1), 1–20 (2001). doi:[10.1006/jath.2000.3565](https://doi.org/10.1006/jath.2000.3565)
3. Bloom, T., Bos, L.P., Calvi, J.P., Levenberg, N.: Polynomial interpolation and approximation in \mathbb{C}^d (2011). <http://arxiv.org/abs/1111.6418>
4. Bojanov, B., Xu, Y.: On polynomial interpolation of two variables. *J. Approx. Theory* **120**(3), 267–282 (2003). doi:[10.1016/S0021-9045\(02\)00023-0](https://doi.org/10.1016/S0021-9045(02)00023-0)
5. Bos, L., De Marchi, S., Caliarì, M., Vianello, M., Xu, Y.: Bivariate Lagrange interpolation at the padua points: the generating curve approach. *J. Approx. Theory* **143**(1), 15–25 (2006). doi:[10.1016/j.jat.2006.03.008](https://doi.org/10.1016/j.jat.2006.03.008)
6. Bos, L., De Marchi, S., Caliarì, M., Vianello, M.: On the Lebesgue constant for the Xu interpolation formula. *J. Approx. Theory* **141**(2), 134–141 (2006). doi:[10.1016/j.jat.2006.01.005](https://doi.org/10.1016/j.jat.2006.01.005)
7. Caliarì, M., De Marchi, S., Vianello, M.: Bivariate polynomial interpolation on the square at new nodal sets. *Appl. Math. Comput.* **165**, 261–274 (2005). doi:[10.1016/j.amc.2004.07.001](https://doi.org/10.1016/j.amc.2004.07.001)
8. Cuyt, A., Benouahmane, B., Hamsapriye, Yaman, I.: Symbolic-numeric Gaussian cubature rules. *Appl. Numer. Math.* **61**(8), 929–945 (2011). doi:[10.1016/j.apnum.2011.03.003](https://doi.org/10.1016/j.apnum.2011.03.003)
9. Gautschi, W.: On inverses of vandermonde and confluent vandermonde matrices. *Numer. Math.* **4**(1), 117–123 (1962). doi:[10.1007/BF01386302](https://doi.org/10.1007/BF01386302)
10. Heinrichs, W.: Improved Lebesgue constants on the triangle. *J. Comput. Phys.* **207**(2), 625–638 (2005). doi:[10.1016/j.jcp.2005.02.002](https://doi.org/10.1016/j.jcp.2005.02.002)
11. Hesthaven, J.S.: From electrostatics to almost optimal nodal sets for polynomial interpolation in a simplex. *SIAM J. Numer. Anal.* **35**(2), 655–676 (1998). doi:[10.1137/S003614299630587X](https://doi.org/10.1137/S003614299630587X)
12. Humberto, R.: On the selection of the most adequate radial basis function. *Appl. Numer. Math.* **33**(3), 1573–1583 (2009). doi:[10.1016/j.apm.2008.02.008](https://doi.org/10.1016/j.apm.2008.02.008)
13. Sauer, T., Xu, Y.: Regular points for lagrange interpolation on the unit disk. *Numer. Algorithms* **12**(2), 287–296 (1996). doi:[10.1007/BF02142808](https://doi.org/10.1007/BF02142808)
14. Sündermann, B.: On projection constants of polynomial space on the unit ball in several variables. *Math. Z.* **188**(1), 111–117 (1984). doi:[10.1007/BF0116387](https://doi.org/10.1007/BF0116387)
15. Szabados, J., Vértesi, P.: *Interpolation of Functions*. World Scientific, Teaneck (1990)
16. Xu, Y.: Funk–Hecke formulae for orthogonal polynomials on sphere and on balls. *Bull. Lond. Math. Soc.* **32**(4), 447–457 (2000). doi:[10.1112/S0024609300007001](https://doi.org/10.1112/S0024609300007001)
17. Xu, Y.: Polynomial interpolation on the unit sphere and on the unit ball. *Adv. Comput. Math.* **20**(1–3), 247–260 (2004). doi:[10.1023/A:1025851005416](https://doi.org/10.1023/A:1025851005416)